INTEGRATING MULTI-MODALITY IMAGING AND BIODYNAMIC MEASUREMENTS FOR STUDYING NECK BIOMECHANICS DURING SUSTAINED-TILL-EXHAUSTION NECK EXERTIONS.

Suman K Chowdhury[1], Ryan M Byrne[1], Yu Zhou[1], Tom Gale[2], Liying Zheng[3], William Anderst[2], Xudong Zhang*[4]

[1]Department of Mechanical Engineering and Materials Science, University of Pittsburgh, Pittsburgh, PA
[2]Department of Orthopaedic Surgery, University of Pittsburgh, Pittsburgh, PA
[3]Health Effects Lab Division, National Institute for Occupational Safety and Health, Morgantown, WV
[4]Department of Industrial and Systems Engineering, Texas A&M University, College Station, TX
*Corresponding Author. Email: xudongzhang@tamu.edu,

Neck musculoskeletal disorders have been associated with various occupational tasks, in particular tasks that require non-neutral sustained exertions. To gain a clear understanding of the neck biomechanics during such exertions, we have recently initiated an unprecedented integration of multi-modality state-of-the-art measurement procedures including dynamic radiographic imaging, surface-based motion capture, electromyography, computed tomography and magnetic resonance imaging. This paper describes an overview of our systematic, integrative efforts of in vivo biodynamic measurements during sustained-till-exhaustion neck exertions and multi-modality imaging data, and how such an integrated database can be used to construct subject-specific neck musculoskeletal models. A complete dataset of one participant is presented to illustrate the acquired data. In the next phase, subject-specific 'what-if' computer simulations will be implemented to understand the mechano-physiological effects of sustained-till-exhaustion neck exertions for different work scenarios and worker characteristics in order to derive effective injury prevention and intervention strategies.

INTRODUCTION

Neck pain is a major health problem with a prevalence rate of 4.9% (332 million people) globally and is the fourth leading cause of years lived with disability (Hoy et al., 2012). It is even more prevalent among workers throughout the industrialized world. For example, from 11 to 14.1% of workers are found to suffer from debilitating neck pain symptoms each year (Côté et al., 2008).

Occupational exposures, such as prolonged sedentary work, awkward postures, repetitive arm and neck movements, and forceful neck exertions are the biomechanical risk factors for neck pain in workers (Côté et al., 2008). Among these risk factors, prolonged, non-neutral neck posture is becoming more prevalent not only in the work environment but also in leisure time with increased dependency on computers and hand-held devices. Thus, neck pain continues to impose a tremendous socio-economic burden as the sedentary trend persists both in the workplace and in the modern lifestyle.

Previous studies have used a broad spectrum of methods ranging from observational, questionnaire, to direct measurement (e.g., electromyography, video- or surface-based measurement) as an attempt to understand the etiology and pathogenesis of neck pain in the occupational setting (Alizadeh et al., 2016; McAtamney & Corlett, 1993; Nimbarte, Zreiqat, & Chowdhury, 2014; Vasavada, Li, & Delp, 2001). Each of these approaches usually focused on one single aspect of the etiology of neck pain. For instance, many of the past studies have empirically evaluated muscle fatigue associated with deviated neck postures using surface-based motion capture and/or electromyography measurements, or have developed biomechanical models to estimate the neck muscle contraction forces. While these studies have confirmed the significant role of neck posture in the biomechanical etiology of occupational neck pain and disorders, a cohesive and accurate description of the structure and function of the neck in vivo during head-neck tasks or exertions has been lacking. In particular, a clear understanding of the simultaneous responses of cervical vertebral bone kinematics and muscle-skeletal dynamics during sustained exertions and how such responses vary across different individuals remains a formidable knowledge gap.

To begin to fill these research voids, we have embarked a systematic effort integrating multi-modality state-of-the-art measurements including dynamic radiographic imaging, surface-based motion capture, electromyography, computed tomography and magnetic resonance imaging to study in vivo neck biomechanics during sustained-till-exhaustion exertions. In this paper, we present an overview of this novel study and describe how we have overcome several challenges in integrating the multiple measurement techniques and succeeded in developing a first-of-its-kind neck biomechanical database. This database will be used in the next phase to develop subject-specific digital human models with high-accuracy musculoskeletal geometry and mechanics for work design and injury prevention as well as intervention purposes.

METHODS

Experimental design

Participants. Forty healthy participants (20 males; 20 females) were recruited to participate in this study. The participants were free from any musculoskeletal discomfort or abnormality and generally in good health at the time of participation, and did not have any prior neck-related disorder,

injury, or surgery. All participants provided written informed consent, approved by the local institutional review board.

Experimental tasks. In this study, participants performed six static sustained-till-exhaustion exertions at their 50% and 100% of maximum voluntary isometric exertion (MVIE) levels in neutral, 40° flexed, and 40° extended head-neck positions. Each task was performed twice. During the tasks, participants pressed their head with an augmented helmet (described in detail below) against a load cell positioned anteriorly during neutral and 40° extended postures, and posteriorly during 40° flexed posture (Figure 1). Audio feedback was provided to maintain the target force level (50% or 100% of MVIE). Prior to the tasks, two exertions at their maximum efforts for 5-10 s were obtained for each posture. The maximum force level of these two exertions was used as the reference to perform the sustained-till-exertion tasks of the corresponding posture. The tasks were randomized across the participants. To reduce the effect of fatigue, sufficient rest period (at least twice the duration of the last trial) was provided between the trials.

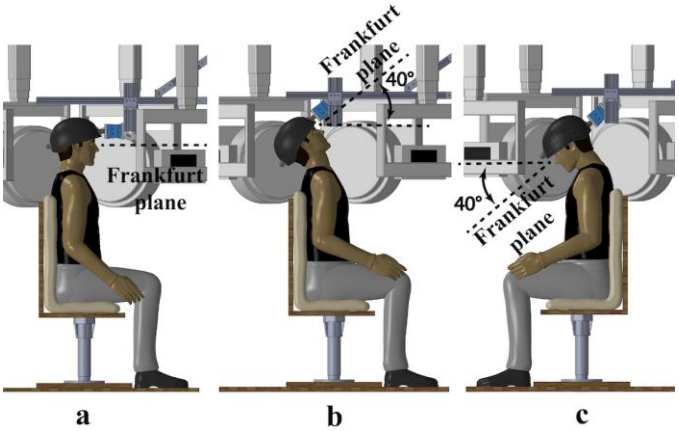

Figure 1: A schematic presentation of a participant performing the exertions at three different head-neck postures: (a) neutral, (b) 40° extended, and (c) 40° flexed.

Data acquisition

Dynamic stereo-radiography (DSX). The DSX system consisted of two cardiac-cine angiography generators (EMD Technologies, CPX-3100CV), two X-ray tubes with 0.3/0.6 mm focal spot, two 16-in Thalus image intensifiers, and two high-speed digital cameras (4-megapixels Phantom v10, Vision Research). X-ray was generated by the cardiac-cine angiography generators (sampling frequency = 30 frames/s; pulsed exposure time = 2.5 ms, excitation voltage = 70 kV, & current = 160 mA). To minimize the radiation exposure, two "snap-shots" were taken: one at the start of exertion, and a second when a subject indicated she or he was exhausted and about to terminate a sustained exertion.

Surface based motion capture system. A 12-camera Vicon motion capture system (Vantage-Series, Vicon Motion Labs, Oxford, UK) was used to record the head-neck postures or motions. The system consists of twelve optical cameras, retro-reflective surface markers (14 mm in diameter), and a data station. Surface markers were placed on ten anatomical locations: the tragion notches, infraorbitales (left and right), glabella, acromion processes (left and right), suprasternal notch, sternum, and C7 spinous process. The marker data was collected continuously at a sampling frequency of 60 Hz for the entire duration of each task. The head-neck flexion-extension angle was measured as the angle between the horizontal plane and Frankfurt plane, defined by surface markers on the tragion notches and infraorbitales (Figure 1). A protractor was used to find the 40° flexed, and 40° extended head-neck positions. The Vicon Nexus 2.2.5 software was used for recording and processing the marker data to compute three-dimensional coordinates.

Surface Electromyography (SEMG) system. The neck muscle activation was measured using Wave Wireless EMG System (formerly known as *ZeroWire* system; Cometa Systems, Italy). The system has fourteen wireless EMG sensors with a band-pass filter of 10-500 Hz. SEMG data was collected with a sampling frequency of 2160 Hz. SEMG data was collected from eight neck muscles: left and right sternocleidomastoid (SCM), left and right hyoid muscles, left and right trapezius (TRAP) muscle at C4-C5 level, and left and right splenius capitis (SPL). Prior to the placements of the snap electrodes, skin underneath the anatomical location of each selected muscle was shaved and cleaned with isopropyl alcohol. The placement of the electrodes was checked for accuracy and cross-talk. The maximum voluntary contraction (MVC) of the muscles were recorded using the procedures suggested by the previous study (Sommerich, Joines, Hermans, & Moon, 2000).

Load cell. A triaxial MTA400 load cell (FUTEK Advanced Sensor Technology, Inc., Irvine, California) was used to measure the neck muscle strength in three directions – X (superior-inferior), Y (medial-lateral), and Z (anterio-posterior) (Figure 2). The load cell had the maximum load capacities of 113 kg, 113 kg, and 226 kg in X, Y, and Z directions, respectively and was calibrated by the manufacturer. The load cell was positioned in a custom designed case in such a way that the Z axis of the load cell laid parallel to the Frankfurt plane of the participants.

Custom-built workstation: A custom-built workstation comprised of an adjustable frame, a height-adjustable chair, and two rails, was used to simulate the dynamic flexion-extension and sustained static exertions at three different head-neck postures (Figure 2). The *adjustable frame* was built using T-slotted aluminum bars (Intek Systems, Inc, Warrendale, PA) of different width and length. The structural design of the frame provided five degrees of freedom: four translations (T1-T4) and one rotation (R1). The adjustability of this frame facilitated three different head-neck postures (neutral, 40° flexion and 40° extension) and accommodated the participants from a broad range of anthropometry. A height-adjustable, cushioned, and 360-degree swivel *chair* was constructed using wood materials. The base of the chair was placed onto two T-slotted metallic *rails* wherein it could be moved forward and backward to adjust the participant within the field of view of the DSX system. The structural design of the chair and the platform provided additional three degrees of freedom: two translations (T5 – T6) and one rotation (R2). A four-strap

harness was used to restrain the torso of the participant throughout the entire tasks.

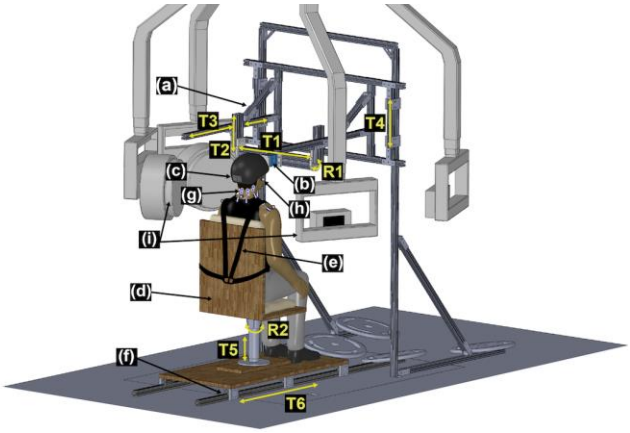

Figure 2: An integrated experimental setup, including: (a) Adjustable frame, (b) load cell, (c) helmet, (d) adjustable chair, (e) strap, (f) rail, (g) SEMG electrodes, (h) surface marker, and (i) DSX system. The workstation has eight degrees of freedom: six translations are denoted as T1 – T6, and two rotations are denoted as R1 – R2.

Daytona half shell helmets (Dennis Kirk, Inc., Rush City, MN) of four sizes – M (head circumference: 53.7-55.9 cm), L (56.2-58.4 cm), XL (58.7-61 cm), 2XL (61.3-63.5 cm) were used to fit a broad range of people. The helmets consisted of sufficient interior padding and chin straps to facilitate participant's head-neck exertions against the load cell. Mounted to the front and back of each helmet was a plastic piece with a spherical protrusion. Such a design allowed the helmet to be accurately positioned and fitted with the spherical cavity of a plate attached to the outer surface of the load cell. The spherical mate was chosen to negate the likelihood of any slipping between the load cell and the helmet surfaces during the forceful head-neck exertions while permitting a quick disengaement.

CT and MRI imaging: A bilateral CT scan (GE Medical Systems Lightspeed Pro 16, Waukesha, WI) from each participant, covering the neck region from C1 to T1 approximately, was acquired at the University of Pittsburgh Medical Center (UPMC) clinical CT facility. The high-resolution MRI scans, head vertex to T3, were also obtained using a 3T clinic scanner (Biograph mMR, Siemens Medical Solutions USA, Inc., PA, USA) at the UPMC Magnetic Resonance Research Center.

Data analysis

The CT and MRI images were segmented in Mimics 17.0 (Materialise Inc., Ann Arbor, MI) to create 3D vertebra and skull skeletal models, respectively. The DSX images were processed using a volumetric model-based tracking technique (Figure 3). This technique has been validated extensively in the previous work (Anderst, Lee, Donaldson, & Kang, 2013). Briefly, the custom software generated a virtual DSX system proportionally and configurationally identical to the actual DSX system (Figure 3). The 3D vertebral bone model reconstructed from CT was placed within the virtual system. Digitally reconstructed radiographs (DRRs) of the vertebral model were created using a ray-tracing algorithm and registered to the experimental DSX dataset. A volumetric image-matching algorithm determined the 3D bone position for each frame such that the correlation between the DRRs and DSX images was maximized. This process was repeated for each cervical vertebral bone.

Using the 3D vertebral models along with the recorded radiographic images during exertion, the model-based tracking procedure produced the 3D, in vivo kinematics at the start and end of each exertion. Figure 4 depicts how the anatomical coordinate systems were defined at each vertebral level. The origin of each vertebra was defined as the centroid of several manually-placed vertebral landmarks. Three orthogonal axes – representing the medial-lateral (X), superior-inferior (Y), and anterior-posterior (Z) directions – were located at the origin (centroid of the vertebra) and followed the right-hand rule. The vertebral kinematics (three rotations: flexion-extension (Rx), twisting (Ry), and lateral bending (Rz); three translations: anterior-posterior (Tz), superior-inferior (Ty), and medial-lateral (Tx)) of the superior (S) vertebra were determined with respect to the inferior (I) vertebra using the Euler principle (Figure 4).

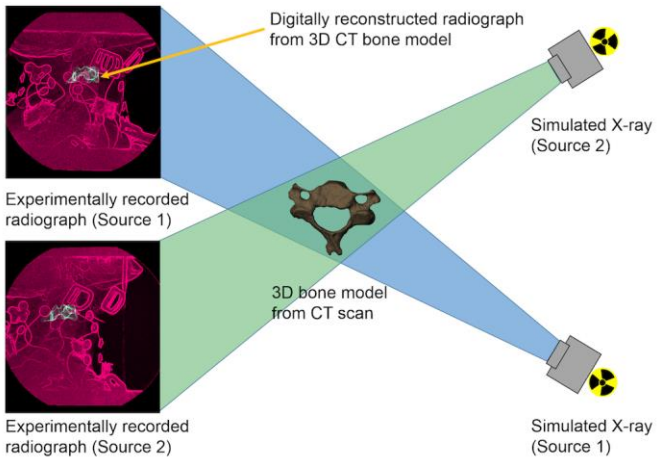

Figure 3: Virtual testing configuration of the DSX system.

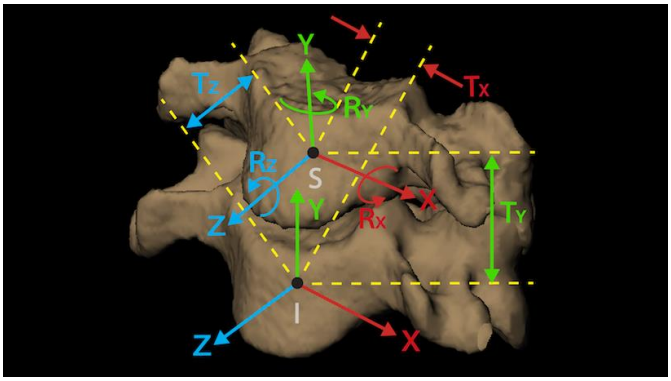

Figure 4: Two adjacent vertebras demonstrating the anatomical directions.

Raw SEMG data were first transferred into frequency domain and passed through a band-pass filter of 10-500 Hz, and a notch filter at 60 Hz and its aliases. The filtered SEMG data were then analyzed in both time and frequency domains. In the time domain, the filtered signals, including the MVC trials, were full-wave rectified, smoothed using a Butterworth

filter of fourth order, and normalized with respect to muscle-specific MVC signals to minimize between-subject or between-muscle errors. In the frequency domain, the filtered signals were analyzed using the fast Fourier transform. A moving window of 0.5s (1080 points) duration (with no-overlapping) was used to estimate the mean absolute value (MAV) and median frequency (MF) in time and frequency domains, respectively. Muscle fatigue was assessed for all sustained with-exertion static trials by estimating the linear correlation coefficient (r) of the MFs at every 5s time interval. The surface marker motion data acquired by the Vicon MX system were tracked and the resulting time series of 3D marker coordinates were organized in accordance with the individual trials performed. The neck flexion-extension angle was estimated for every data point of the entire trial. Similarly, the load cell data was also tracked, and smoothed using a Butterworth filter of fourth order and a moving average window of 50ms.

RESULTS

A complete dataset of one participant (male; age: 28; height: 167 cm; weight: 70 kg) is presented to illustrate the results that are currently being generated from the data processing procedures.

The mean activation level for an entire sustained-till-exhaustion trial is presented in Table 1. The extensor muscles (e.g. Trap and SPL muscle groups) showed higher activations compared to flexor muscles (e.g. SCM and Hyoid muscle groups) since the participant performed a 'extension' exertion at 40° flexed head-neck posture. On the contrary, the flexor muscles demonstrated higher activations compared to the extensor muscles since the participant performed 'flexion' exertion during both 40° extended and neutral postures. Majority of the muscles showed negative trends during the sustained exertions and were more prominent at the non-neutral postures; complementing the notion that a sustained-till-exhaustion task at a non-neutral posture may result in more muscular imbalance than the sustained-till-exhaustion task at a neutral posture (Table 2).

Table 1: The mean absolute value (in percent) of the SEMG data. The 40° extended and 40° flexed neck postures are denoted by 40° E and 40° F, respectively.

	50% of MVIE			100 % of MVIE		
Muscles	40° E	Neutral	40° F	40° E	Neutral	40° F
Right SCM	27.4	17.2	1.7	48.8	42.1	3.2
Left SCM	28.7	24.9	3.1	49.6	42.9	7.4
Left Trap	2.8	2.2	24.1	4.4	2.9	54.0
Right Trap	1.6	1.7	50.5	2.8	2.2	34.6
Right SPL	14.8	10.1	18.4	25.7	19.7	41.0
Left SPL	9.9	8.8	17.5	23.2	17.8	51.4
Right Hyoid	24.9	10.5	1.2	40.6	29.3	1.6
Left Hyoid	26.7	23.5	1.6	55.8	40.4	2.4

The C1-C2 vertebral flexion-extension kinematics for the start and end positions of the exertions are presented in Table 3. The changes in cervical kinematics at all C1-C7 levels during the sustained-till-exhaustion task at 50% of MVIE are illustrated in Figure 5. An initial inspection indicates there may be observable changes in the cervical kinematics due to the fatiguing though grossly static exertions.

Table 2: The correlation coefficient values of the MF trends. A negative value represents a decrease in median frequency.

	50% of MVIE			100 % of MVIE		
Muscles	40° E	Neutral	40° F	40° E	Neutral	40° F
Right SCM	-0.56	-0.39	-0.64	-0.84	-0.41	-0.45
Left SCM	-0.33	-0.20	-0.23	-0.35	-0.74	-0.66
Left Trap	-0.47	-0.46	-0.15	-0.62	-0.75	-0.73
Right Trap	-0.68	-0.15	-0.10	-0.30	-0.89	-0.70
Right SPL	-0.59	0.01	-0.15	-0.68	-0.06	-0.70
Left SPL	-0.38	-0.27	-0.06	0.42	-0.55	-0.78
Right Hyoid	-0.52	-0.16	-0.51	-0.91	-0.76	-0.78
Left Hyoid	-0.48	-0.23	-0.45	-0.60	-0.66	-0.49

Table 3: Cervical vertebral kinematic data at C1-C2 level. The units of the rotational and translational data are degree and mm, respectively.

	40° E		Neutral		40° F	
	Start	End	Start	End	Start	End
Rx (°)	-24.05	-25.29	-24.99	-24.87	-11.13	-9.68
Ry (°)	0.55	0.73	3.26	3.70	1.95	3.72
Rz (°)	-2.43	-2.25	-2.14	-2.54	-1.99	-2.12
Tx (mm)	-0.75	-0.66	-0.12	0.16	0.35	0.43
Ty (mm)	16.38	16.65	16.91	16.78	17.38	17.27
Tz (mm)	-7.30	-7.36	-6.30	-6.32	-5.79	-6.31

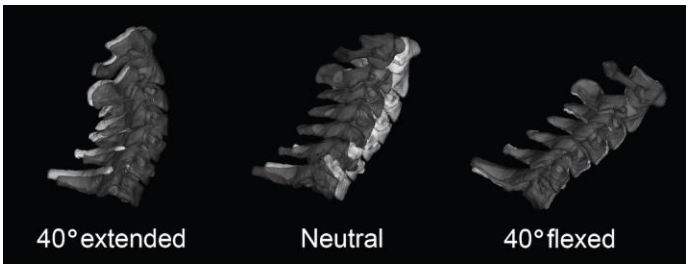

Figure 5: Superimposed cervical spine sagittal views at the start (grey) and end (silver) of 50% MVIE trials at three different postures.

For a conclusive insight of the neck mechanics during sustained-till-exhaustion exertion, the database contains subject-specific neck muscular and skeletal geometry. Figure 6 depicts the locations and cross-sectional areas of the individual muscles at C2 and C5 levels. The individual neck muscles were portrayed with different colors on each MRI slice to retrieve subject-specific information such as skull volume, origin and insertion point of each muscle, individual muscle volume, the total neck morphometry, and so on.

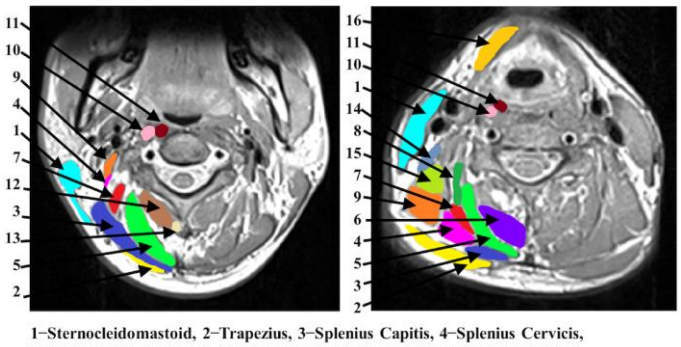

Figure 6: MRI scans with two slices at C2 (left) and C5 (right) levels. Individual muscles are portrayed with different colors.

DISCUSSION

In this study, four different types of biodynamic measurements including bi-plane dynamic radiography (X-ray) of cervical spine, surface-based head-neck kinematics, neck muscle activation using electromyography, and neck muscle strength using a triaxial load cell were acquired while participants performed sustained-till-exhaustion tasks. In addition, the participants underwent CT and MR imaging procedures. One distinct notion is that we are studying sustained exertions, which are conventionally considered as static exertions, as dynamic activities so that we can discern subtle but important time-dependent changes. In the next phase, we will construct subject-specific musculoskeletal biomechanical models based on the biodynamic data in conjunction with the CT and MR imaging data.

We are using OpenSim (Delp et al., 2007), an open-source musculoskeletal modeling platform, to construct subject-specific musculoskeletal models. The generic model will be calibrated using subject-specific passive properties of the joint from MR data by minimizing the net moment differences (errors) from two types of simulations – inverse dynamics and EMG-driven forward dynamics (Figure 7). The calibration process will tune subject-specific passive joint properties and thus reconcile the discrepancies between the model-predictions and experimental measurements.

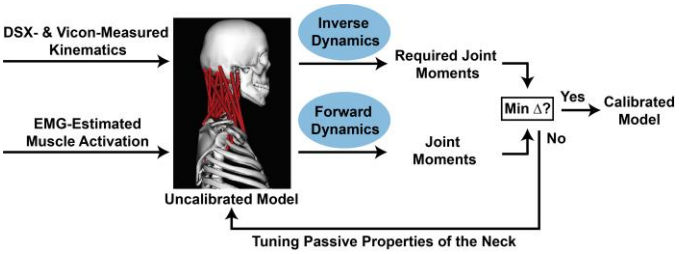

Fig 7: Logic diagram of the calibration process to construct a subject-specific neck biomechanical model. Delta (Δ) denotes the discrepancies in the joint moments.

In the inverse dynamic simulation, although the accurate kinematics (e.g. DSX and Vicon measured kinematics) is modeled as input, the predicted muscle activations inevitably have discrepancies with the EMG-estimated activations. Similarly, the predicted kinematics in the forward dynamics is not the same as the DSX and Vicon measured kinematics. The predicted joint compressive forces between adjacent vertebrae from C1-C2 to C6-C7 using both inverse and forward dynamic approaches will be estimated for all tasks at the beginning and the end of the exertion, and then will be compared and evaluated about disc deformation data (Figure 8).

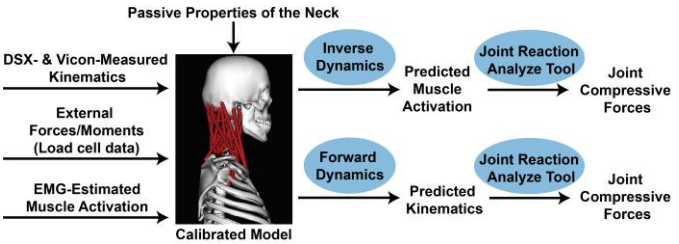

Fig 8: Logic flow diagram for the model-based inverse and forward dynamics analysis.

The biodynamic measurements and multi-modality imaging data alone cannot be used to directly address the mechano-physiological effects of sustained-till-exhaustion neck exertions. However, they are essential to calibrating a generic musculoskeletal model and thus attaining a subject-specific or "personalized" model along with accurate estimates of neck joint compressive forces and other tissue mechanical responses. In that regard, the subject-specific musculoskeletal biomechanical models not only are built based on the biodynamic and imaging data but also serve to integrate them with a clear logic. This logic will be the underpinning for design or simulation of scenarios that do not yet exist or are experimentally not testable.

ACKNOWLEDGEMENT

The work was funded by a research grant (R01OH010587) from the Centers for Disease Control and Prevention/National Institute for Occupational Safety and Health (CDC/NIOSH).

REFERENCES

Alizadeh, M., Knapik, G., Dufour, J., Zindl, C., Allen, M., Bertran, J., & Marras, W. (2016). An EMG-driven biomechanical model of the canine cervical spine. *Journal of Electromyography and Kinesiology*.

Anderst, W. J., Lee, J. Y., Donaldson, W. F., 3rd, & Kang, J. D. (2013). Six-degrees-of-freedom cervical spine range of motion during dynamic flexion-extension after single-level anterior arthrodesis: comparison with asymptomatic control subjects. *J Bone Joint Surg Am, 95*(6), 497-506. doi: 10.2106/JBJS.K.01733

Côté, P., van der Velde, G., Cassidy, J. D., Carroll, L. J., Hogg-Johnson, S., Holm, L. W., . . . Hurwitz, E. L. (2008). The burden and determinants of neck pain in workers. *European Spine Journal, 17*(1), 60-74.

Delp, S. L., Anderson, F. C., Arnold, A. S., Loan, P., Habib, A., John, C. T., . . . Thelen, D. G. (2007). OpenSim: open-source software to create and analyze dynamic simulations of movement. *IEEE transactions on biomedical engineering, 54*(11), 1940-1950.

Hoy, D., Bain, C., Williams, G., March, L., Brooks, P., Blyth, F., . . . Buchbinder, R. (2012). A systematic review of the global prevalence of low back pain. *Arthritis & Rheumatism, 64*(6), 2028-2037.

McAtamney, L., & Corlett, E. N. (1993). RULA: a survey method for the investigation of work-related upper limb disorders. *Applied ergonomics, 24*(2), 91-99.

Nimbarte, A. D., Zreiqat, M. M., & Chowdhury, S. K. (2014). Cervical flexion–relaxation response to neck muscle fatigue in males and females. *Journal of Electromyography and Kinesiology, 24*(6), 965-971.

Sommerich, C. M., Joines, S. M., Hermans, V., & Moon, S. D. (2000). Use of surface electromyography to estimate neck muscle activity. *Journal of Electromyography and Kinesiology, 10*(6), 377-398.

Vasavada, A. N., Li, S., & Delp, S. L. (2001). Three-dimensional isometric strength of neck muscles in humans. *Spine, 26*(17), 1904-1909.